UNIVERSITY OF COLORADO BOULDER

HONORS THESIS

Gas Cherenkov Muon Monitor for the DUNE Neutrino Oscillation Experiment

by

Max Weiner

Reviewed by:

Professor Alysia Marino, Advisor, Physics

Professor Paul Beale, Honors Council Representative, Physics

Professor Mark Rast, Astrophysical and Planetary Sciences

April 6, 2018

UNIVERSITY OF COLORADO BOULDER

Abstract

Gas Cherenkov Muon Monitor for the DUNE Neutrino Oscillation Experiment

by Max WEINER

The upcoming Deep Underground Neutrino Experiment will begin to take data in the 2020s and will be capable of making the most precise measurements of neutrino oscillation parameters which will help answer some of the most fundamental questions in physics today. In order to accomplish this task, it is essential to know the neutrino flux at both the near and far detectors. To aid in this difficult measurement will be a system of muon monitors to characterize the associated muon beam. This paper concentrates on measuring the muon distribution at the beginning of the beam with a gas Cherenkov detector with the goal of constraining the neutrino energy and momentum distribution. Currently there is a prototype detector at the Fermi National Accelerator Laboratory in the NuMI beamline that makes these measurements. We attempt to extrapolate a muon distribution by observing and analyzing these signals over various gas pressures and detector orientations. I will discuss how such a model is created and how to go about comparing the simulations with real data as well as what future work is necessary.

Acknowledgements

I would like to acknowledge my deepest gratitude to those who have offered me their support and guidance throughout this research project. First, and foremost, I want to thank Alysia Marino for being such an outstanding adviser and leader. She has put aside countless hours educating and navigating me since I started here over two years ago. Her enthusiasm and passion for what is experimental neutrino physics is truly contagious. I cannot thank her enough for turning me on to such a fascinating field and for helping me along with this project, and more. I would also like to thank Jeremy Lopez, without whom this thesis would not have been possible. Jeremy helped me develop the complicated computer code used for this research. The entire Neutrino Group has been nothing but a pleasure to work with. Finally, I want to thank my committee members, Paul Beale and Mark Rast, for taking the time to participate in my honors research project.

Contents

List of Figures

List of Tables

Chapter 1

Introduction

In this paper I will summarize my research in the past year-and-a-half which involves a muon monitoring system for the future Deep Underground Neutrino Experiment. This work involved recording and analyzing data as well as helping develop a fitter so as to compare real data with simulations.

Chapter One introduces the Standard Model of particle physics as well as the history of neutrinos and their importance to physics today. Next, the Deep Underground Neutrino Experiment is introduced along with its science goals and how it will accomplish these goals. Chapter Two discusses Cherenkov radiation and how it is utilized in particle physics. The relevance of a gas Cherenkov detector for neutrino physics is revealed in this chapter. Chapter Three details how to build a model which predicts a muon flux with a gas Cherenkov detector. Chapter Four is the conclusion and future work needed to further this project.

1.1 Neutrinos and The Standard Model of Particle Physics

The Standard Model (SM) of particle physics is the theoretical framework which describes elementary particles and their interactions. Within this

framework is a tiny neutral particle called the neutrino which has been baffling scientists since it was first postulated to exist in 1930 [1]. This conflict between the SM and the neutrino eluding a complete understanding suggests neutrinos may light the way to a more fundamental theory of nature beyond the SM.

1.1.1 Standard Model

The Standard Model of particle physics describes matter at its most fundamental level. It postulates that the universe is composed of a handful of matter and antimatter particles as well as force-carrying particles (see Figure 1.1). The matter particles are spin-$\frac{1}{2}$ fermions and are divided into leptons and quarks while the force-carriers are spin-1 and spin-0 gauge bosons. The leptons are further divided into three generations according to their flavor: e, μ, and τ. Each flavor forms a pair containing a charged lepton (l) and an associated neutral particle, a neutrino (ν_l).

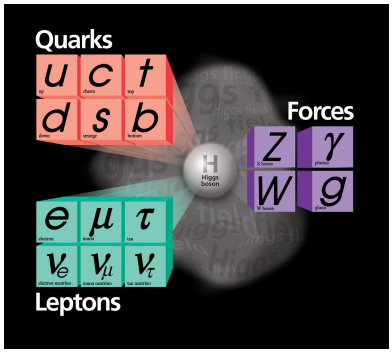

FIGURE 1.1: List of particles in the Standard Model. Particles are grouped into force particles (purple), leptons (green), quarks (red), and the Higgs boson (grey). Not shown are each particle's antimatter counterpart.

The SM was developed in the 1970s and has successfully explained almost all experimental results and predicted a wide variety of phenomena [2]. It describes all of the four fundamental forces: electromagnetism, the weak

force, the strong force, and gravity[1]. Each force has a particle which is in charge of mediating that interaction: the strong force is carried out by gluons, the weak force is mediated by the W and Z bosons, gravity interacts via the graviton, and the electromagnetic force is governed by the photon. Forces manifest via the exchange of force particles (e.g. a photon is exchanged between two electrons when they repel one another). The quarks experience all four forces while the leptons are invisible to the strong force altogether. All leptons feel the weak force, and because neutrinos have zero charge they do not interact electromagnetically. It has been established that neutrinos have a tiny mass, about one millionth the mass of the electron [3]. Neutrinos are special in that their most significant interaction is comes from the weak force, and here their interaction range is minuscule ($\sim 10^{-18}$ m) due to the W and Z bosons being so heavy ($\sim$90 GeV/c^2). This combination of being neutral, having a tiny mass, and a minuscule interaction range makes neutrino detection formidable. In the next section I will explain what a neutrino is and the problems it presents to the SM.

1.1.2 Neutrinos

What is a neutrino and how does it conflict with the SM? Neutrinos were first hypothesized in 1930 by Wolfgang Pauli to save the laws of conservation of energy and momentum in β decay [1]. Radioactive nuclei will have a neutron decay into a proton and emit an electron (historically known as a β particle). The expected outcome was that in each decay an electron of constant energy would be emitted; the electron's energy being the difference between the initial and final energies of the nucleus. Surprisingly, a continuous spectrum of electron energies was measured. Where was the missing energy? Some (including Niels Bohr [3]) claimed this was proof that the law

[1] Although gravity is included in the SM, along with its hypothetical force particle the graviton (not included in Figure 1.1), an adequate quantum theory of gravity compatible with general relativity has not yet been established.

of conservation of energy is wrong. Pauli suggested that an undetectable, tiny, neutral particle must be carrying off the missing energy and momenta (later named the neutrino). Soon after, Enrico Fermi put together a relativistic quantum field theory describing β decay which incorporated neutrinos. But it wasn't until decades later, in 1956, when Frederick Reines and Clyde Cowan confirmed their existence by detecting antineutrinos via inverse β decay ($\overline{\nu}_e + p \rightarrow n + e^+$) at the Savannah River nuclear plant in South Carolina [1].

The theoretical models assumed neutrinos came in three flavors (ν_e, ν_μ, and ν_τ) and were massless because they travel at a speed indistinguishable from the speed of light [4]. In the 1960s, Ray Davis studied solar neutrinos with a giant underground detector at the Homestake Mine in Lead, South Dakota. The Sun undergoes nuclear fusion and thus emits an extraordinary number of neutrinos ($\sim 10^{12}$ pass through your body every second, day and night!) yet Davis detected only about one third of the predicted neutrinos [5]. What was wrong? Were the theorists incorrect or was their something awry in Davis' measurements? This is what is now known as the "Solar Neutrino Problem." It turns out Davis' detector (a tank containing 100,000 gallons of dry cleaning fluid) was only sensitive to measure electron neutrinos. The physicists Bruno Pontecorvo, Ziro Maki, Masami Nakagawa, and Shoichi Sakata [6, 7] proposed that neutrinos undergo oscillations (i.e. an electron neutrino can suddenly transform into a muon neutrino) but this can only happen if neutrinos have mass. Neutrino oscillations weren't confirmed until within the last couple of decades by the Super-Kamiokande (1998) and Subdury Neutrino Observatories (2002) whose discovery was awarded the Nobel Prize in 2015.

1.1.3 Neutrino Oscillations

What are neutrino oscillations and why are they important? Neutrino flavor states are not equivalent to neutrino mass eigenstates. Instead, they are superpositions of the mass eigenstates ν_1, ν_2, and ν_3:

$$|\nu_l\rangle = \sum_{i=1}^{3} U_{li}^{*} |\nu_i\rangle , \quad l = e, \mu, \tau \tag{1.1}$$

and so the masses of the flavor states are not well defined. The matrix U is the Pontecorvo-Maki-Nakagawa-Sakata (PMNS) Matrix:

$$\begin{aligned} U &= \begin{pmatrix} U_{e1} & U_{e2} & U_{e3} \\ U_{\mu 1} & U_{\mu 2} & U_{\mu 3} \\ U_{\tau 1} & U_{\tau 2} & U_{\tau 3} \end{pmatrix} \\ &= \begin{pmatrix} 1 & 0 & 0 \\ 0 & c_{23} & s_{23} \\ 0 & -s_{23} & c_{23} \end{pmatrix} \begin{pmatrix} c_{13} & 0 & s_{13}e^{-i\delta_{CP}} \\ 0 & 1 & 0 \\ -s_{13}e^{i\delta_{CP}} & 0 & c_{13} \end{pmatrix} \begin{pmatrix} c_{12} & s_{12} & 0 \\ -s_{12} & c_{12} & 0 \\ 0 & 0 & 1 \end{pmatrix} \end{aligned}$$

and c_{ij} and s_{ij} are shorthand for $\sin(\theta_{ij})$ and $\cos(\theta_{ij})$. The mixing angles θ_{ij} relate the amount of mass eigenstates in each flavor state and the Dirac CP violation phase δ_{CP} suggests neutrinos and antineutrinos oscillate differently for a nonzero value (neutrinos mix by U, antineutrinos mix by the complex conjugate U^{*}).

To illustrate the oscillatory behavior of neutrinos, let us assume that there are only two flavor states and two mass states. Then we can write our flavor states as [8],

$$|\nu_e\rangle = \cos\left(\frac{\theta}{2}\right)|\nu_1\rangle + \sin\left(\frac{\theta}{2}\right)|\nu_2\rangle$$
$$|\nu_\mu\rangle = \sin\left(\frac{\theta}{2}\right)|\nu_1\rangle - \cos\left(\frac{\theta}{2}\right)|\nu_2\rangle$$

where θ is the parameter describing the mixing between flavor and mass states. So if we have an electron neutrino as our initial state, what is the probability of measuring it to be a muon neutrino at some later time t? Neutrino flavor states are eigenstates of the weak interaction, whereas the mass states are the eigenstates of the free-particle Hamiltonian [9]. Thus, the electron neutrino evolves in time (in vacuum) according to the Schrödinger equation,

$$|\psi(t)\rangle = \cos\left(\frac{\theta}{2}\right)e^{-iE_1t/\hbar}|\nu_1\rangle + \sin\left(\frac{\theta}{2}\right)e^{-iE_2t/\hbar}|\nu_2\rangle$$

and the probability of measuring a muon neutrino is given by,

$$\begin{aligned} P_{\nu_e\to\nu_\mu} &= |\langle\nu_\mu|\psi(t)\rangle|^2 \\ &= \frac{\sin^2(\theta)}{4}|1 - e^{-i(E_2-E_1)t/\hbar}|^2 \\ &= \sin^2(\theta)\sin^2\left(\frac{(E_2-E_1)t}{2\hbar}\right). \end{aligned}$$

In the relativistic limit where the neutrinos are traveling at near the speed of light,

$$E_i \approx pc + \frac{(m_ic^2)^2}{2pc},$$
$$p \approx E/c,$$
$$t \approx L/c.$$

Thus,

$$P_{\nu_e \to \nu_\mu} = \sin^2(\theta) \sin^2\left(\frac{(m_2^2 - m_1^2)Lc^3}{4E\hbar}\right). \tag{1.2}$$

Equation 1.2 applies to neutrinos in vacuum, corrections must be applied when they travel through matter.

The full three neutrino probability function is more complicated,

$$\begin{aligned} P(\nu_l \to \nu_{l'}) =& \delta_{ll'} - 4\sum_{i>j} Re(U_{li}^* U_{l'i} U_{lj} U_{l'j}^*) \sin^2\left(\frac{\Delta m_{ij}^2 L}{4E}\right) \\ &+ 2\sum_{i>j} Im(U_{li}^* U_{l'i} U_{lj} U_{l'j}^*) \sin^2\left(\frac{\Delta m_{ij}^2 L}{2E}\right), \end{aligned}$$

where $\Delta m_{ij}^2 = m_i^2 - m_j^2$. The main idea is the same for both cases: the oscillatory nature depends on the parameter L/E, where all other variables are constant. As you can see from the oscillation equations, only Δm_{ij}^2 can be measured, not the absolute value of the neutrino masses. These masses remain unknown, in fact it is a question of whether the masses fall into a normal hierarchy ($m_1 < m_2 < m_3$) or an inverted hierarchy ($m_3 < m_1 < m_2$) as shown in Figure 1.2. Long-baseline neutrino experiments measure these oscillation parameters by shooting a neutrino beam to a large detector hundreds of kilometers away. This, along with solar neutrino and nuclear reactor experiments, has resulted in the best-fit values as shown in Table 1.1. The Deep Underground Neutrino Experiment is one such project that will, among other things, make the most precise measurement of the CP violation parameter δ_{CP}. This is an important measurement as it may explain the matter/antimatter asymmetry of the observable universe.

CP violation is the notion that under both charge conjugation (changing

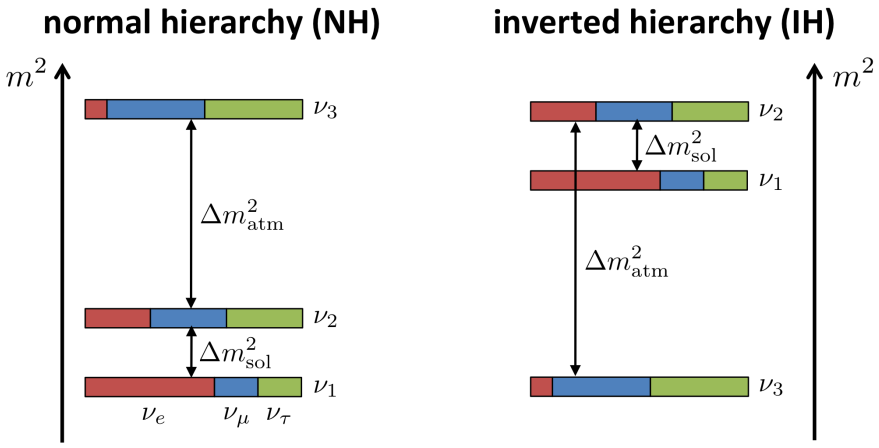

FIGURE 1.2: Illustration of normal and inverted hierarchies. Only difference of mass squares can be measured via neutrino oscillations, not absolute masses. Colors represent amount of flavor in each mass state.

a particle to its antiparticle) and parity (inverting spatial coordinates), particles do not behave symmetrically. So far, only left-handed neutrinos and right-handed antineutrinos have been observed [3]. This means that neutrinos maximally violate charge conjugation and parity separately, yet it is unknown if neutrinos violate the combination, CP. If we act CP on a left-handed neutrino:

$$\begin{aligned} CP\,|\nu_L\rangle &= C\,|\nu_R\rangle \\ &= |\overline{\nu_R}\rangle\,. \end{aligned}$$

So if the state $|\nu_L\rangle$ oscillates differently than $|\overline{\nu_R}\rangle$, then neutrinos violate CP symmetry. Since it is a complex phase, the sign of δ_{CP} is different for neutrinos and antineutrinos and a nonzero (as well as non-π) value manifests itself in different oscillatory behavior. CP violation has been observed for quarks but never for leptons. It is in this respect that neutrinos may explain the matter/antimatter asymmetry of the observable universe (the mixing of quarks

TABLE 1.1: Current best-fit values on neutrino oscillation parameters[12]. Values are given as: normal hierarchy (inverted hierarchy) and $\Delta m^2 = m_3^2 - (m_2^2 + m_1^2)/2$.

Parameter	**Best-Fit**	**3σ**
$\Delta m^2_{21}[10^{-5}eV^2]$	7.37	6.93 - 7.97
$\lvert\Delta m^2\rvert[10^{-3}eV^2]$	2.50 (2.46)	2.37 - 2.63 (2.33 - 2.60)
$\sin^2(\theta_{12})$	0.297	0.250 - 0.354
$\sin^2(\theta_{23})$	0.437 (0.569)	0.379 - 0.616 (0.383 - 0.637)
$\sin^2(\theta_{13})$	0.0214 (0.0218)	0.0185 - 0.0246 (0.0186 - 0.0248)
δ_{CP}	Unknown	

is too small to explain this asymmetry).

1.2 The Deep Underground Neutrino Experiment

The Deep Underground Neutrino Experiment (DUNE), utilizing the Long-Baseline Neutrino Facility (LBNF), is an upcoming long-baseline neutrino project. DUNE will make the most precise measurements of the oscillation parameters as well as address the following big questions [10]

1. **Matter/Antimatter Asymmetry.** Equal parts matter and antimatter were created in the Big Bang but we live in a universe of matter. What explains this asymmetry? A possible explanation is a value of the CP violating phase $\delta_{CP} \neq 0$ or π. This would be the first evidence of CP violation in the lepton sector. It is observed in the quark sector but is not enough to explain the matter/antimatter asymmetry of our universe.

2. **Nature's Fundamental Underlying Symmetries.** Insight into new symmetries beyond the Standard Model can be gained by measuring the

mixing parameters, determining the ordering of the neutrino masses, and understanding how this relates to the analogous quark mixings.

3. **Grand Unified Theories (GUTs).** Theories that encapsulate all of the forces predict protons should decay, which DUNE will be sensitive enough to measure.

4. **Supernovae.** When stars explode they release an intense burst of neutrinos. Measuring this phenomena will help further understand how stars collapse.

The world's most intense neutrino beam will be fired from the Fermi National Accelerator Laboratory (FNAL) near Batavia, Illinois 1300 km to the Sanford Underground Research Facility (SURF) in Lead, South Dakota (Figure 1.3) [11]. The far site neutrino detector will be a multi-kiloton liquid argon time projection chamber (LArTPC) housed at SURF approximately one mile underground (to shield from cosmic rays in our atmosphere). The advantage of having a giant detector and high-intensity beam is a high event rate, which is essential for neutrino experiments since they hardly interact. DUNE will be the longest baseline neutrino experiment which will aid in measurements of δ_{CP} and the determination of the neutrino mass ordering [10].

1.2.1 Long-Baseline Neutrino Facility

LBNF will provide the infrastructure for DUNE including the neutrino beam, a beam monitoring system, as well as the near and far sites which will house the near and far detectors. These facilities will be located at Fermilab (near site) or SURF (far site). The far site will host the LArTPC far detector while the near site will be home to the beam, beam monitoring system, and near detector.

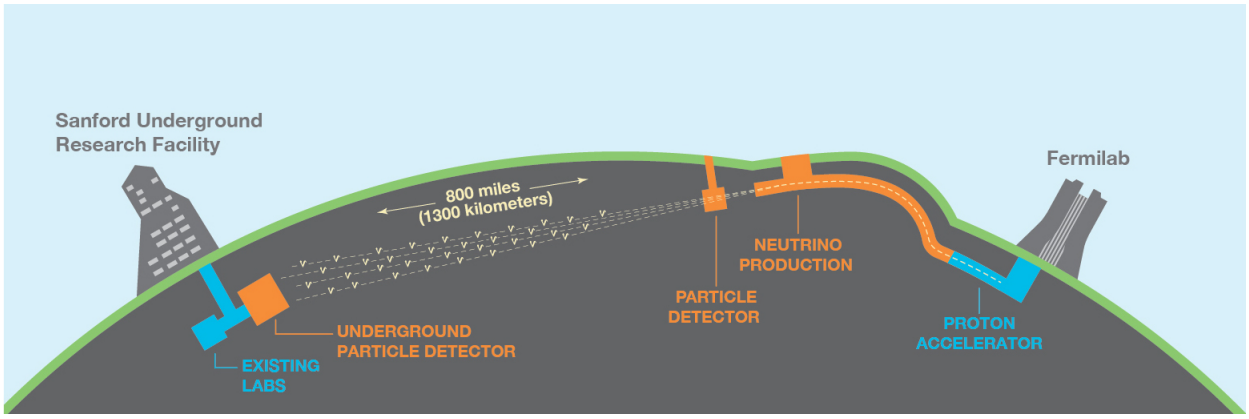

FIGURE 1.3: A neutrino beam will be fired from Fermilab in illinois 1300 km to the Sanford Underground Research Facility in Lead, South Dakota.

Near Site Facilities

The neutrino beam is created by accelerating protons to high energies (60 to 120 GeV) by a series of accelerators and colliding them into a target creating charged hadrons (mostly pions with some kaons). The pions and kaons are focused with a series of electromagnetic horns into a 200 meter pipe where a large fraction decay into muons and muon neutrinos. The magnetic horn focuses for either positive or negative charges depending on the direction of the current and thus can select for a neutrino or antineutrino beam:

$$\pi^+ \rightarrow \mu^+ + \nu_\mu$$
$$\pi^- \rightarrow \mu^- + \bar{\nu}_\mu.$$

The resulting neutrinos and their associated muons continue in the same direction where they encounter a hadron absorber designed to capture any remaining baryons or mesons. Neutrinos pass straight through to the near and far detectors. Muons do make it through the absorber, but not much farther.

A system of monitors are set up in alcoves just beyond the absorber to measure these muons. An illustration of this process is shown in Figure 1.4.

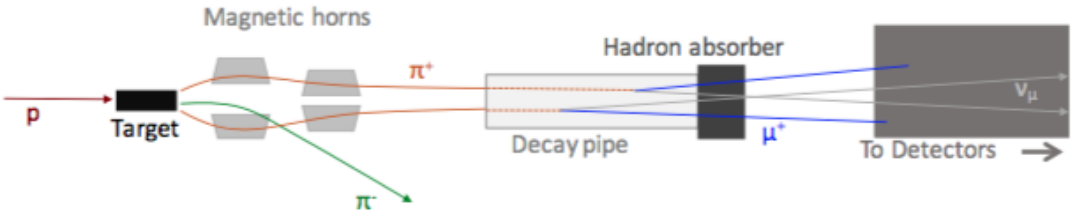

FIGURE 1.4: High-energy protons collide with a fixed target producing (mostly) charged pions. The direction of the horn's current selects for either positive or negative pions which correspond to a neutrino or antineutrino beam. The selected pions are focused into a 200 meter pipe where they each decay into one muon and one neutrino. Any remaining hadrons are subtracted by the absorber, the muons travel as far as the alcoves, and the neutrinos make the journey to the far detector.

The near detector will be stationed near the origin of the neutrino beam (beyond the alcoves) and will measure the beam's initial flux and energy spectrum. There are, however, uncertainties in the interaction rates and neutrino event rates are small. Muons don't suffer this problem, the changes in the beam can be seen much more quickly with muon monitors. This is also a nice independent cross check of the beam flux from the near detector. To measure the oscillation parameters it is crucial to understand the initial energy distribution and flavor composition of the neutrino beam. In addition, data from the near detector will be used to measure neutrino interaction cross sections.

1.2.2 Far Detector

The far detector is located 1300 km from the beam at SURF and will consist of four 17 kiloton liquid argon time projection chambers (LArTPC) 1.5 km underground [10]. The detectors are underground to shield against any

background noise from cosmic rays in our atmosphere. By the time the neutrinos arrive at the far detector from the near site ($\sim$0.004 seconds) they will have travelled mostly uninterrupted through Earth's crust. They will enter the LArTPC and undergo weak interactions ultimately producing a signal.

Time projection chambers are volumes with a constant electric field maintained by a series of anode and cathode wire planes. The electric field is in the transverse direction relative to the beamline. Each volume will be filled with liquid argon, which must be kept below $\sim -186^{\circ}C$ in order to stay a liquid. Neutrinos will undergo a weak interaction with an argon nucleus producing a charged lepton dictated by the neutrino's flavor as well as transmutating the argon atom. The charged byproducts will create ionized electrons which will drift to the detection planes. Combining these detections with timing information enables a three-dimensional reconstruction of the particle tracks.

Although most neutrinos undergo zero interactions on their way to the far detector, their oscillations are affected as they travel through Earth. In fact, neutrinos and antineutrinos are affected differently. This matter effect typically inhibits measurements of δ_{CP}; DUNE, due to its large baseline (1300 km), will be able to resolve this issue and measure δ_{CP}.

Chapter 2

Gas Cherenkov Muon Monitor

In this chapter I will overview the physics of Cherenkov radiation and how it can be applied to experimental particle physics. I will then describe the specific detector that has been studied for this thesis.

2.1 Cherenkov Radiation

Pavel Cherenkov won the 1958 Nobel Prize in physics for the discovery that charged particles moving in a medium faster than light emit electromagnetic radiation [13]. This phenomenon is called Cherenkov radiation. A charged particle moving through a dielectric medium with index of refraction n polarizes the molecules in the medium. Once the particle has passed, the molecules return to their unpolarized state by emitting photons. If the particle's velocity is greater than the speed of light in that medium ($v > c/n$) the result is constructive interference of Cherenkov radiation as a coherent wavefront at an angle θ_c relative to the particle's trajectory (Figure 2.1) [9].

The light is emitted in a cone, much like shockwaves are sent out in a cone when a jet travels faster than the speed of sound, and is characterized by the Cherenkov angle θ_c. From this geometrical relationship we see that $\cos(\theta_c) = 1/n\beta$. We can derive the particle's momentum threshold p_T, the minimum momentum a particle must have to undergo Cherenkov radiation. Note that $\cos(\theta_c)$ is bounded above by one, which means at threshold $v_T = c/n$ and,

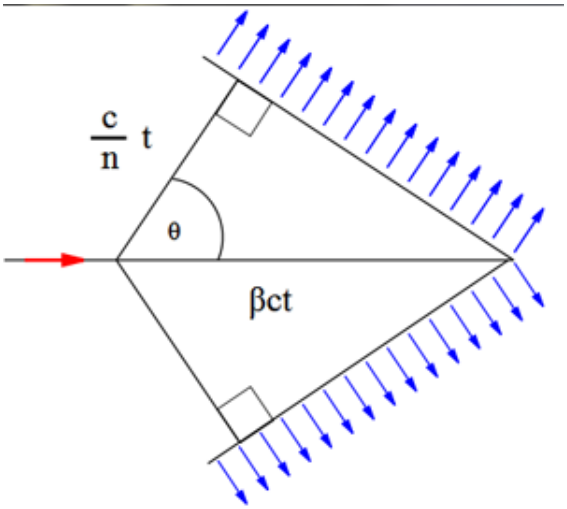

FIGURE 2.1: A charged particle traveling in a medium with index of refraction n emits light in a cone at the Cherenkov angle, θ_c. The particle and photon travel a distance βct and ct/n, respectively, where $\beta = \frac{v}{c}$.

$$p_T = \gamma m v_T$$
$$p_T = \frac{mc}{n\sqrt{1-\beta^2}}$$
$$p_T = \frac{mc}{\sqrt{n^2-1}}.$$

Therefore, only a particle of momentum $p > p_T$ will produce Cherenkov radiation. For some experiments, this fact is exploited to help identify particles of momentum p: only particles with mass

$$mc < (n^2-1)^{1/2} p$$

will emit Cherenkov raditation. Further, the number of photons produced per unit length (via this process) is given by the Frank-Tamm formula [12]

$$\frac{dN}{dx} = \int \frac{2\pi\alpha z^2}{\lambda^2}\left(1 - \frac{1}{\beta^2 n^2(\lambda)}\right) d\lambda$$

$$= 2\pi\alpha z^2 \sin^2(\theta_c) \int_{\lambda_1}^{\lambda_2} \frac{d\lambda}{\lambda^2}$$

where z is the charge of the incoming particle, α is the fine structure constant, n is the index of refraction as a function of photon energy, and the photon wavelength is integrated over values for which $\beta > 1/n(\lambda)$. The intensity of the emitted light grows with frequency, this is why nuclear reactors make water glow blue (blue and violet being the highest frequency the eye can detect). The number of radiated photons also grows with the Cherenkov angle; particles near the momentum threshold will emit very little light.

Cherenkov detectors can be utilized in different ways for neutrino physics. The Super-Kamiokande experiment in Japan is a 50 kiloton water Cherenkov detector. The water is in a large cylindrical volume with thousands of photo-mulitplier tubes (PMTs) lining the inside walls. A neutrino will undergo an elastic scattering interaction producing a super-luminal electron. This electron emits Cherenkov radiation which is detected as rings by the PMTs. This is called ring-imaging and the number of detected photons provides a measure of the neutrino energy while the direction of the electron can be determined from the orientation of the Cherenkov ring (Figure 2.2) [9].

The detector discussed in this paper consists of a pipe filled with argon gas. Its ability to pivot relative to the beamline and adjust the gas pressure (i.e. change n) offers the potential to constrain the muon (and ultimately the neutrino) beam profile as I will discuss next.

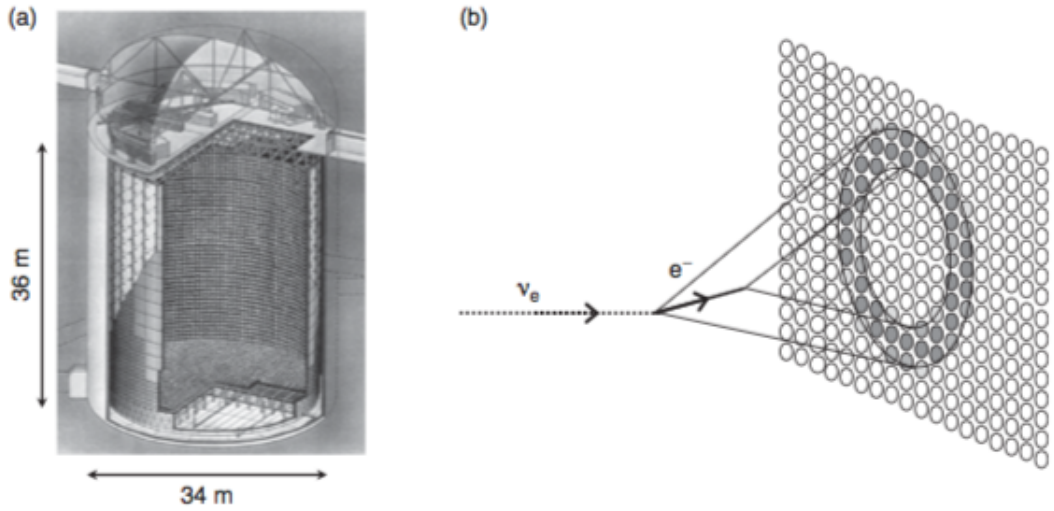

FIGURE 2.2: (a) Schematic of the Super-Kamiokande water tank and (b) illustration of ring-imaging from an electron neutrino event. Photo from *Modern Particle Physics* by Mark Thomson. [9]

2.2 Gas Cherenkov Detector

The detector used for this project consists of an L-shaped chamber filled with argon gas (Figure 2.3). It is located in the NuMI beamline at Fermilab. NuMI (Neutrinos at the Main Injector) is an existing facility which provides a neutrino beam pointed to detectors in northern Minnesota. Attached at the elbow is a mirror and at the end of the leg perpendicular to the beamline is a photo-multiplier tube (PMT) which counts the number of photons. The PMT is sensitive to the visible spectrum (300 to 700 nm). Charged particles (in our case, muons) enter the one-meter-long leg along the beamline and emit photons at some angle θ_c. Photons are then reflected towards the PMT. The perpendicular leg is long ($\sim$5 m) to filter out any noise from the high radiation of the beam (it is important that our signal comes only from Cherenkov radiation due to the beam). The fact that the muons emit photons at some angle θ_c which must strike the mirror and be perfectly reflected to hit the PMT make this design sensitive to muon momentum and incident angle, detector orientation, as well as the pressure of the gas. The detector is allowed

to move in pitch (0.828° to 6.011°) and yaw (-6.064° to 4.695°) via actuators. The gas inside the chamber is allowed to vary in pressure (0 to 200 psi) which in turn changes the index of refraction n.

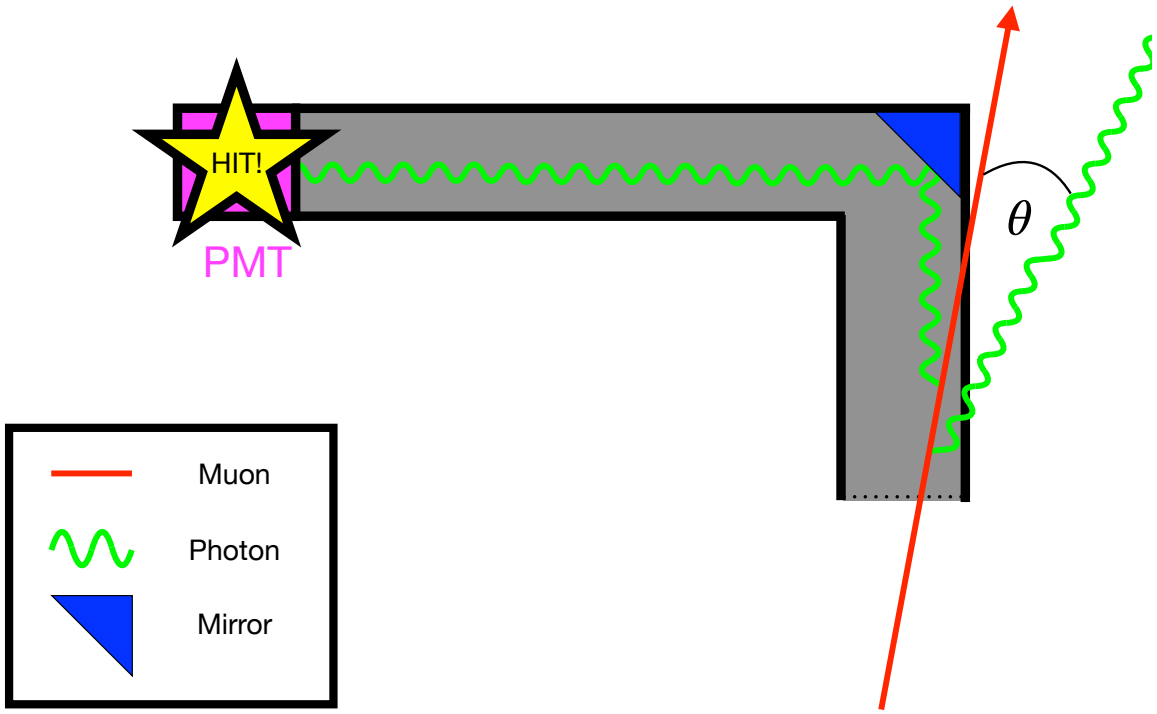

FIGURE 2.3: A detector filled with argon gas designed to measure Cherenkov radiation from a muon beam (red). Muons enter the argon medium and undergo Cherenkov radiation (green) which reflect off the mirror (blue) to be recorded by a PMT.

We have been taking data from the gas Cherenkov detector in the NuMI beamline (Figure 2.4). It is located in Alcove 2, approximately 14 meters downstream from the hadron absorber (Figure 2.5). It is roughly centered with the beamline. One application of this device is to monitor beam stability. Since muons and their neutrinos are produced in a one-to-one ratio and (for the most part) share the same direction, a measurement of the muon beamline is a good approximation of the neutrino beamline; their energies

are correlated in the two body decays ($\pi \rightarrow \mu\nu$). Using data from the detector, profiles of the beam were created (shown in Figure 2.6). Note the signal is negative; a large signal corresponds to a more negative value. This is because the PMTs read out a negative voltage due to the photoelectric effect. This is a nice check to see that the beam is running properly. We can also point to where the beam deviates and, from being aware of what was going on at the time, what the cause was (Figure 2.7).

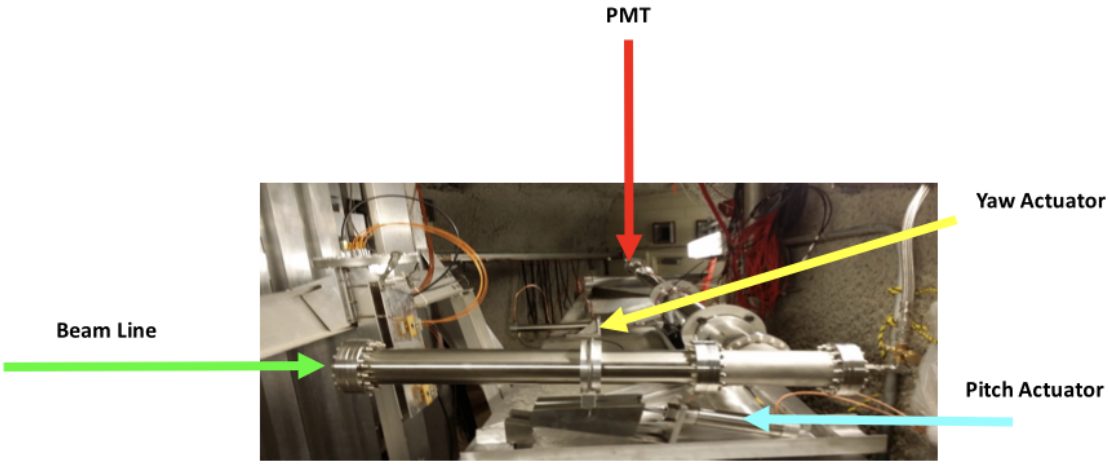

FIGURE 2.4: This is the gas Cherenkov detector currently in the NuMI beamline at Fermilab located in Alcove 2. It is operational and the data is used to monitor beam stability. It will also be used to extrapolate the flux of the muon beam by performing pressure scans.

In the next chapter I will discuss further utility of a gas Cherenkov detector; specifically, how it can be used to extrapolate a muon distribution of the beam. This information will help constrain the flux of the neutrino beam.

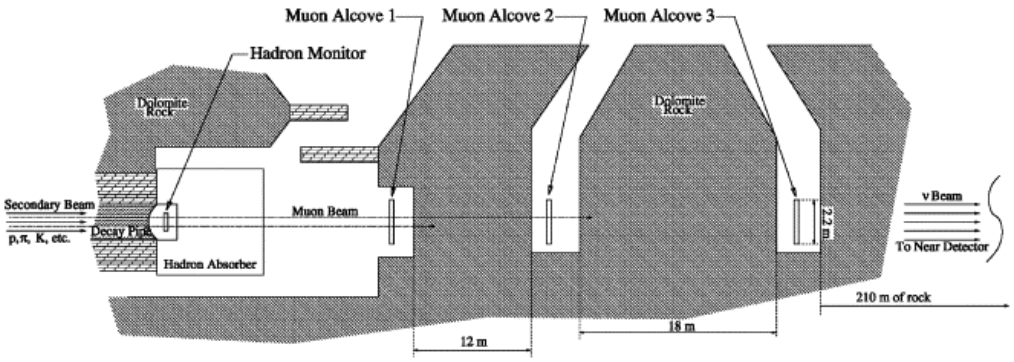

FIGURE 2.5: Top view of particle beam from end of decay pipe through muon alcoves. Undecayed hadrons are absorbed after decay pipe, leaving a beam of muons and neutrinos. Neutrinos travel through unhindered to near and far detectors while muons are measured before being absorbed by Earth.

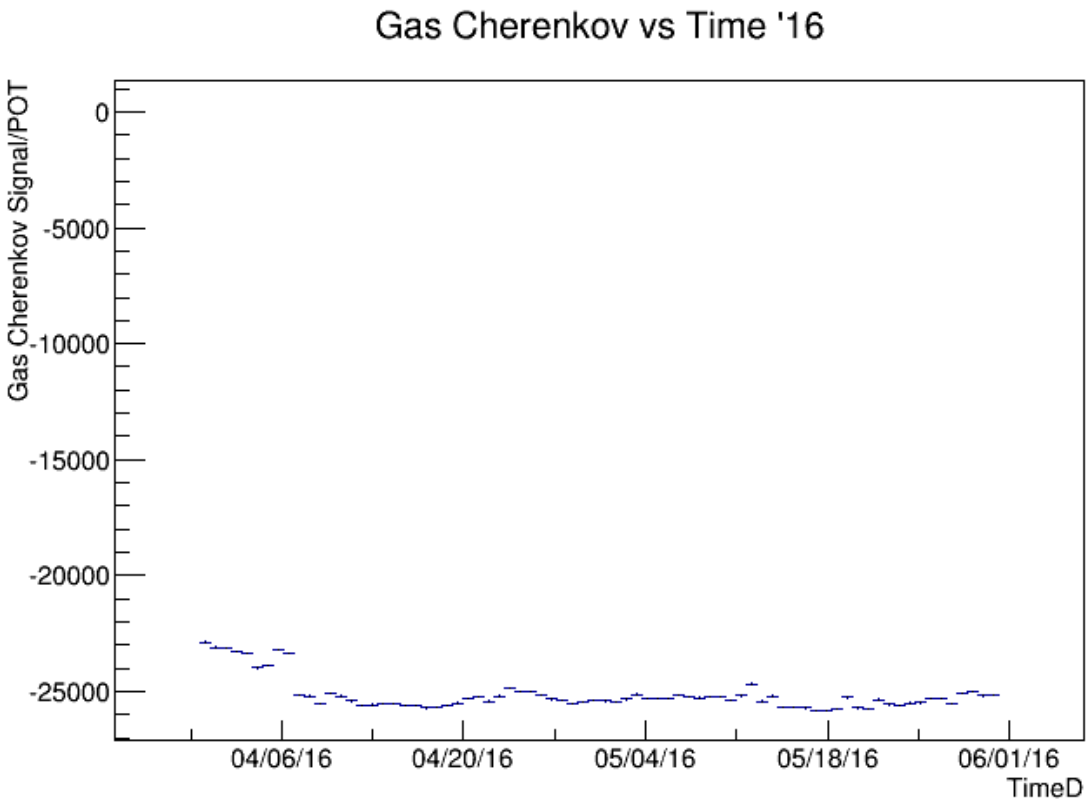

FIGURE 2.6: Here is a profile of a relatively stable muon beam. This is used as a nice, and quick, check to ensure the neutrino beam is operating as expected.

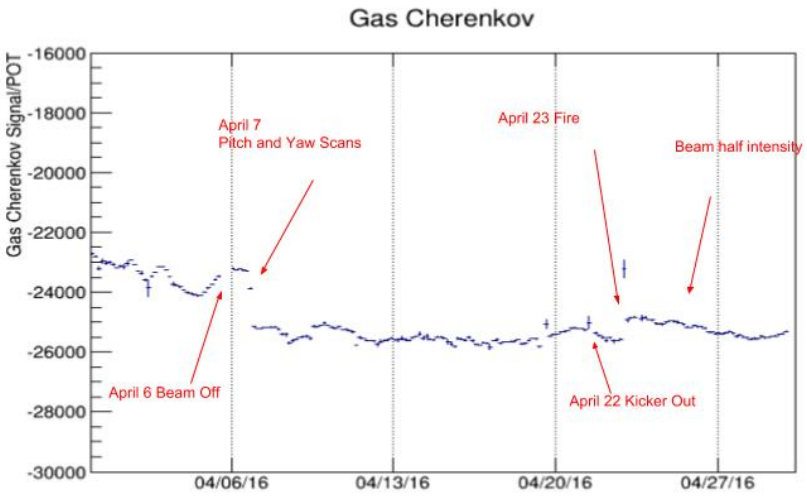

FIGURE 2.7: This is a profile of an "erratic" muon beam labeled with events to explain such behavior.

Chapter 3

Predicting a Muon Distribution

In this chapter I will discuss how to develop a model to predict a muon distribution (in momentum and direction) utilizing a gas Cherenkov detector and what future work will be needed to accomplish this task. The general idea is that particular muon distributions will generate unique signals in our detector over various pressures and yaws (the signals are like a "finger print" of some muon distribution). Our goal then is to extrapolate, or constrain, the muon beam distribution by observing the subsequent signal from a gas Cherenkov detector over various orientations and pressures (look at output signal and reconstruct muon distribution in momentum and direction). This in turn will help constrain the associated neutrino distribution. This model is computationally intensive and I will show how time-consuming Monte Carlo simulations can be significantly shortened.

3.1 Pressure Scans at NuMI

The first step was to take data with the gas Cherenkov detector in the NuMI beamline over several yaws and pressures. The detector was operated remotely from Boulder, Colorado and the pitch was fixed to be (roughly) centered with the beamline. We took data over seven pressures (8, 16, 32, 60, 100, 150, and 200 psi) and let the yaw vary from approximately -5 to 3 degrees relative to the beamline center. Data was taken from a neutrino

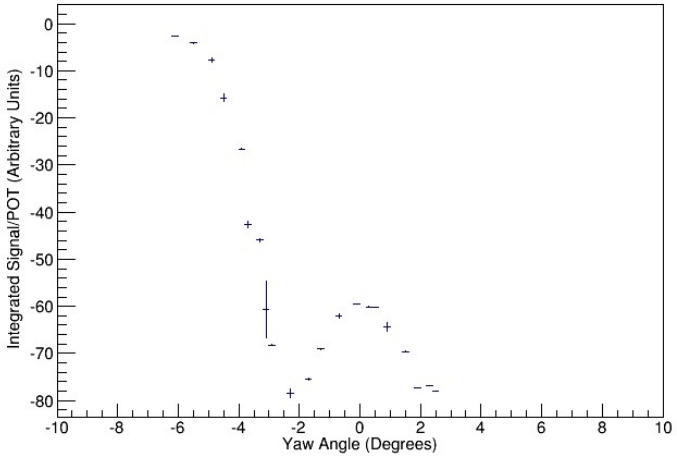

(A) Yaw scan taken at 60 psi.

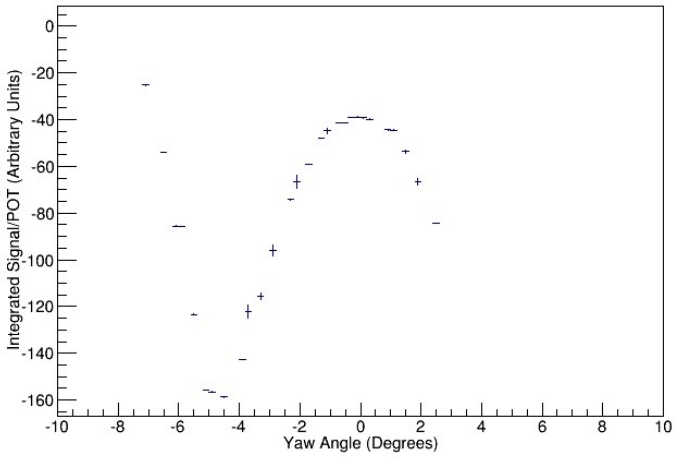

(B) Yaw scan taken at 200 psi.

FIGURE 3.1: Yaw scans taken during neutrino mode (i.e. antimuon beam) at 60 and 200 psi. Note the signal reads out from a negative voltage; a more negative value corresponds to a larger signal.

(and later from an antineutrino) beam shown in Figure 3.1. The plots show the integrated signal per protons on target (POT) versus the detector's yaw orientation which is measured in degrees relative to the beamline center (note that a more negative value means a larger signal).

The signal grows and makes a more pronounced "W" shape at higher pressures. This makes sense: Cherenkov radiation, as well as the number of photons radiated per muon, depends on the particle's momentum and the index of refraction n of the medium (which is related to pressure). We know

that only high momentum muons will contribute to the signal at low pressures [14],

$$p_T = \frac{mc}{\sqrt{n^2-1}}, \qquad n(P) = (n_{Ar} - 1) \times \left(\frac{P}{14.7 \text{ atm}}\right) + 1$$

where n_{Ar} is the index of refraction of argon at λ ~400 nm, and P is the pressure of the argon inside the detector in pounds per square inch (psi). Note that n grows with pressure.

The "W" shape makes sense because the detector is highly sensitive to the Cherenkov angle; the largest signals will occur where the Cherenkov angle is "just right" relative to the muon's incident angle and detector orientation. The signal is symmetric relative to the beamline center because light is radiated in a cone. At larger pressures the momentum threshold decreases and more muons will exhibit Cherenkov radiation. A greater Cherenkov angle (which increases with pressure for a given muon momentum) also means the number of emitted photons per muon will increase according to the Frank-Tamm formula; these factors explain the larger signal and more pronounced "W" at higher pressures.

3.2 Monte Carlo Simulations

These plots can be recreated with Monte Carlo simulations using the computer program Geant4, a platform designed to simulate particles through matter an ubiquitously used throughout the particle physics community. Using the same pressures that were used with the detector at Fermilab, pressure scans were performed over similar yaw angles in half-degree increments (Figure 3.2). The muon flux in the decay pipe used for this recreation came from a beam simulation. The muons were then simulated through a gas

Cherenkov detector in Alcove 2 and a "signal" was produced by counting the number of photons hitting the PMT. As is shown in Figure 3.3, we were able to produce the same shapes generated from the real detector. More simulations (statistics) would probably result in a better shape.

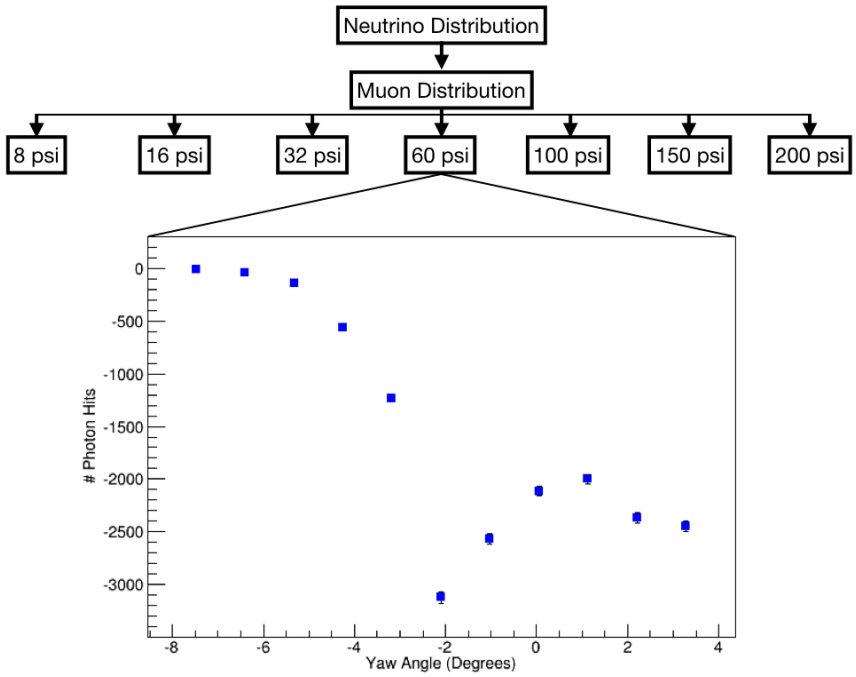

FIGURE 3.2: An initial distribution of neutrinos in the decay pipe was obtained from a beam simulation. This was converted into a muon distribution via conservation of energy and momentum. Yaw scans were then performed over seven different pressures and eleven yaw orientations each. Each blue square corresponds to a Monte Carlo simulation involving over one million muons and takes approximately two hours to run.

The simulations accurately describe our setup at NuMI. But how do we extrapolate a muon distribution from a signal? Well, we will ultimately have to fit a simulated signal to the real signal by adjusting the muon distribution. This is in essence extremely time consuming: simulate a large number of muons through the detector about 70 times (seven pressures and ten yaw orientations), see if the signal agrees with the real output, if not adjust muon distribution and repeat until they match, then you have found your distribution. Simulating one million muons for a single configuration takes about

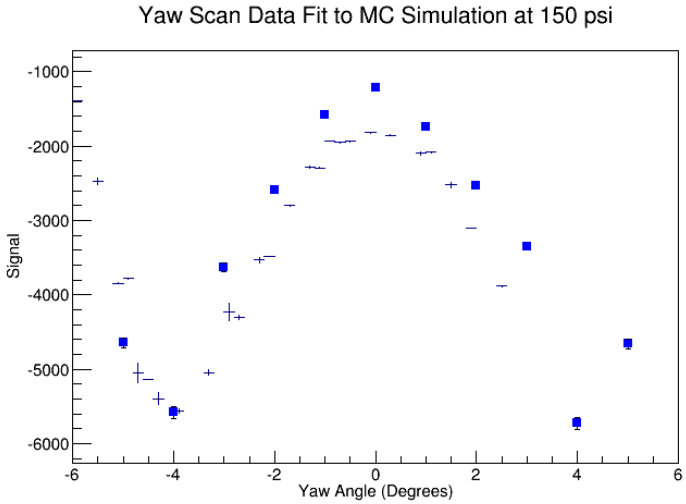

(A) Yaw Scan at 150 psi.

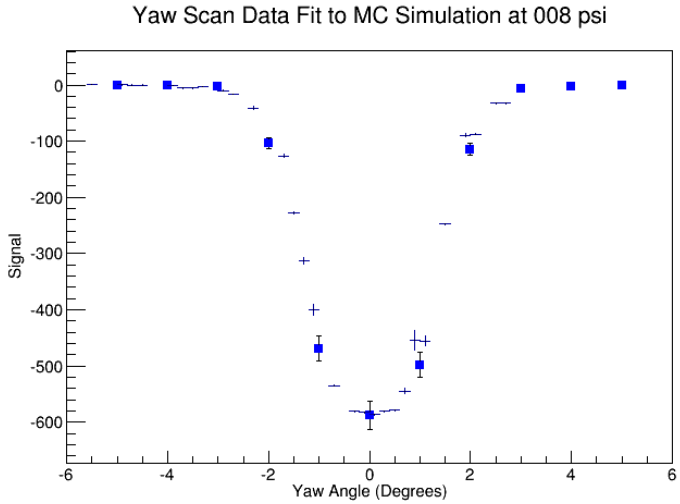

(B) Yaw Scan at 8 psi.

FIGURE 3.3: These plots show that yaw scans from Monte Carlo simulations (dark blue squares) recreate the same shape taken with real data (blue crosses).

two hours, so time adds up quickly (could run in parallel, still long).

To reduce the computing time, we decided to build a four-dimensional yield matrix. For a given muon momentum and direction (p, θ) as well as detector configuration in yaw and pressure (Y, P), our yield matrix assigns each muon a "hit" or signal. To build this matrix we ran simulations over discrete values in (p, θ, P, Y):

$p =$ (1, 2, 4, 8, 12, 18) GeV

$\theta =$ (0.1, 0.5, 1, 1.5, 2, 2.5, 3, 3.5, 4, 4.5, 5) degrees from beam center

$P =$ (8, 16, 32, 60, 100, 150, 200) psi

$Y =$ (0.5, 1, 1.5, 2, 2.5, 3, 3.5, 4, 4.5, 5) degrees from beam center.

This comes out to 4,620 files with 100,000 muons in each file. This allowed us to build a matrix in (p, θ)-space such that for some detector configuration in yaw and pressure, we can assign each muon a "signal" based on the muon's momentum and direction as shown in Figure 3.4. The signal we create with the yield matrix sums over all muon momenta and direction for a given pressure and yaw,

$$\text{Signal}(P, Y) = \sum_{p,\theta} N_\mu(p, \theta) \times YM(p, \theta, P, Y)$$

where N_μ is the number of muons as a function of p and θ and is the important parameter we are attempting to extract (we want the N_μ that produces the signal which best matches our data). The function YM is our four-dimensional yield matrix in charge of assigning a signal. Although the matrix is built from discrete values, we can assign any muon a number of hits (signal) via interpolation. If we find that we are low on statistics, or resolution in (p, θ), we can always run more muons per file (or add more values of p and θ). Comparing the time it takes to output a signal via Monte Carlo simulations (which takes on the order of hours for one million muons) with this yield matrix technique (assigns a signal in a matter of minutes) it is easy to appreciate the advantages of the latter method.

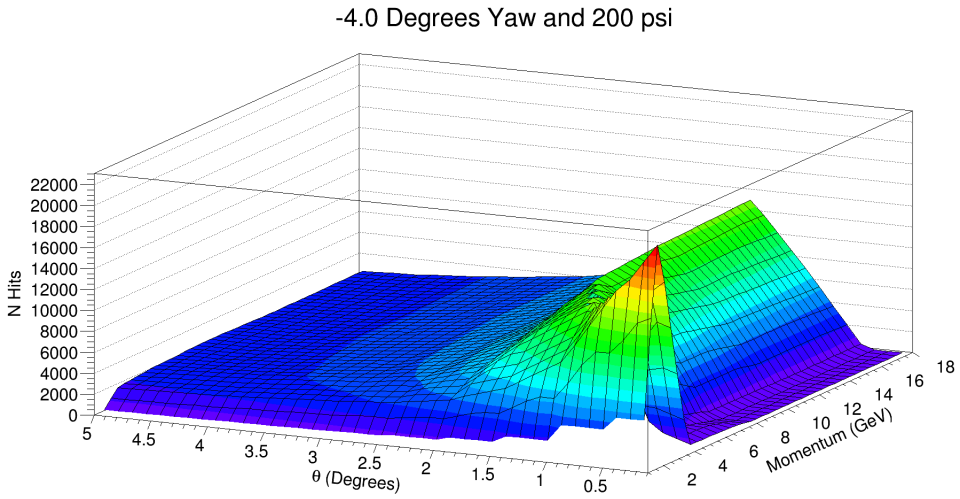

FIGURE 3.4: Yield matrix in (p, θ)-space at 200 psi and yaw of -4°. The z-axis is the number of photon detections (or hits) which correspond to an output signal. Although this matrix was built with discrete values of p and θ, muons with intermediate values are assigned a signal via interpolation.

Using the yield matrix is a quick way of creating a signal for a large number of muons, but we still have yet to predict a muon distribution. To do this, I created a function fitted to the "realistic" distribution file from NuMI (Figure 3.5). The end result is a distribution that says the number of muons as a function of momentum and direction is,

$$N_\mu(p,\theta) = \left(a(p)\theta + b(p)\theta^2 + c(p)\theta^3 + d(p)\theta^4\right) \times 2.2^{-\theta/\sigma(p)} \tag{3.1}$$

where the coefficients of the polynomial of θ are functions of the muon's momentum (and so is the exponent). The function was then fitted over several momentum regimes (divided in such a way that each regime had approximately the same number of muons) shown in Figures 3.6 and 3.7. Each regime resulted in different parameters, and we fitted for the parameters themselves (Figure 3.8).

The end result is the following eight parameter function,

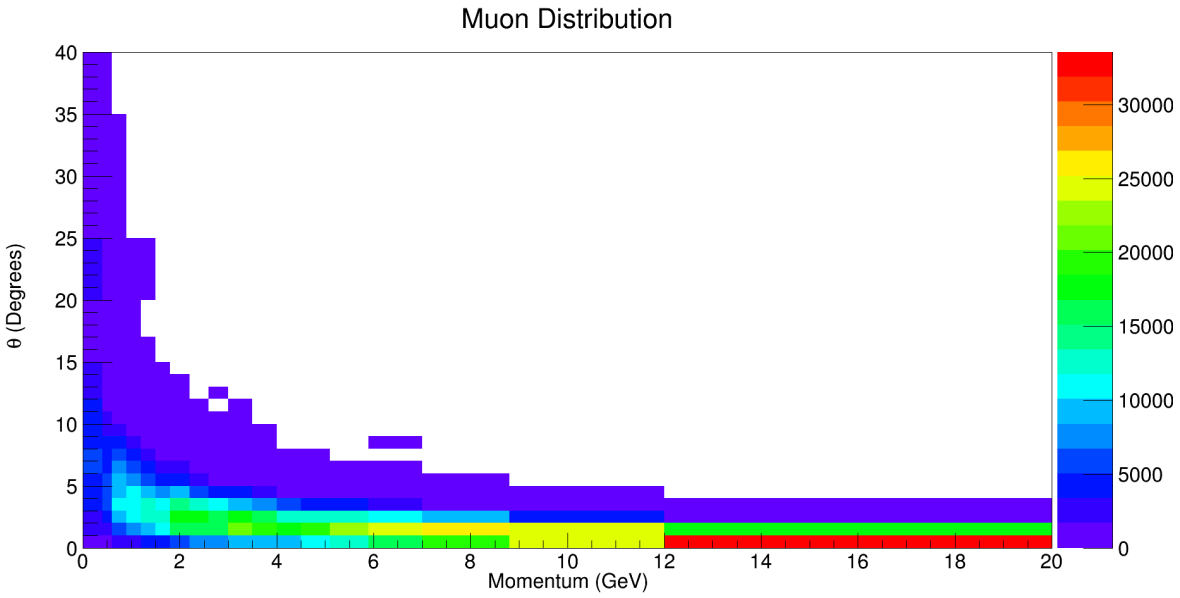

FIGURE 3.5: Muon distribution used to run Monte Carlo simulations. The colors indicate the number of muons in each bin according to the particle's momentum and direction, θ. Most muons have an angle less than 5° off from beamline center.

$$
\begin{aligned}
N_\mu(p,\theta) = \Big(& ([0]p + [1]p^3)\theta \\
& + ([2]p^2 + [3]p^3)\theta^2 \\
& + ([4]p^2 + [5]p^3)\theta^3 \\
& + ([6]p^2 + [7]p^3)\theta^4 \Big) * 2.2^{-\theta * 0.558p}
\end{aligned}
\tag{3.2}
$$

Shown below in Figure 3.9 are plots of simulated yaw scans using the same distribution of 100,000 muons distributed according to Equation 3.2. There are two output signals, one generated the long way with Geant4, and the short way using the yield matrix. The disagreement is the largest where the signal is the biggest (most negative). The error can probably be reduced with a higher resolution in (p, θ) for the yield matrix.

To demonstrate that a muon distribution is capable of being extrapolated from a yaw scan, Figure 3.10 shows how the signal changes when the parameters in Equation 3.2 are altered. If there was more time, a fitter would have

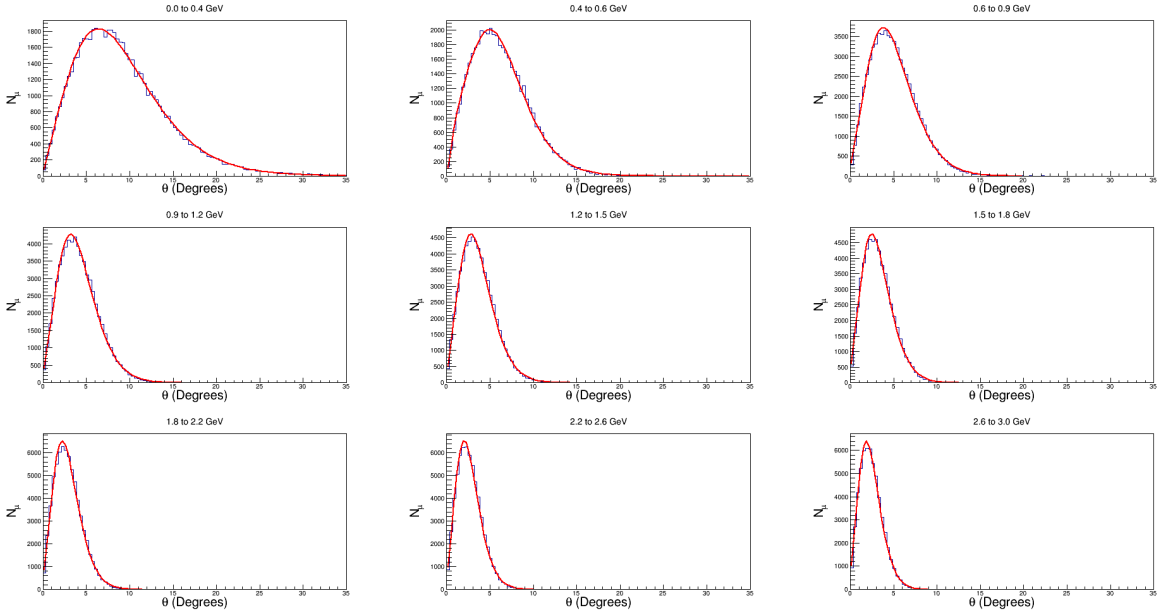

FIGURE 3.6: Number of muons vs θ in different momentum ranges.

been constructed to match an output signal with a best-fit muon distribution. The ultimate goal is to fit for the parameters in 3.2 to data (the output signal).

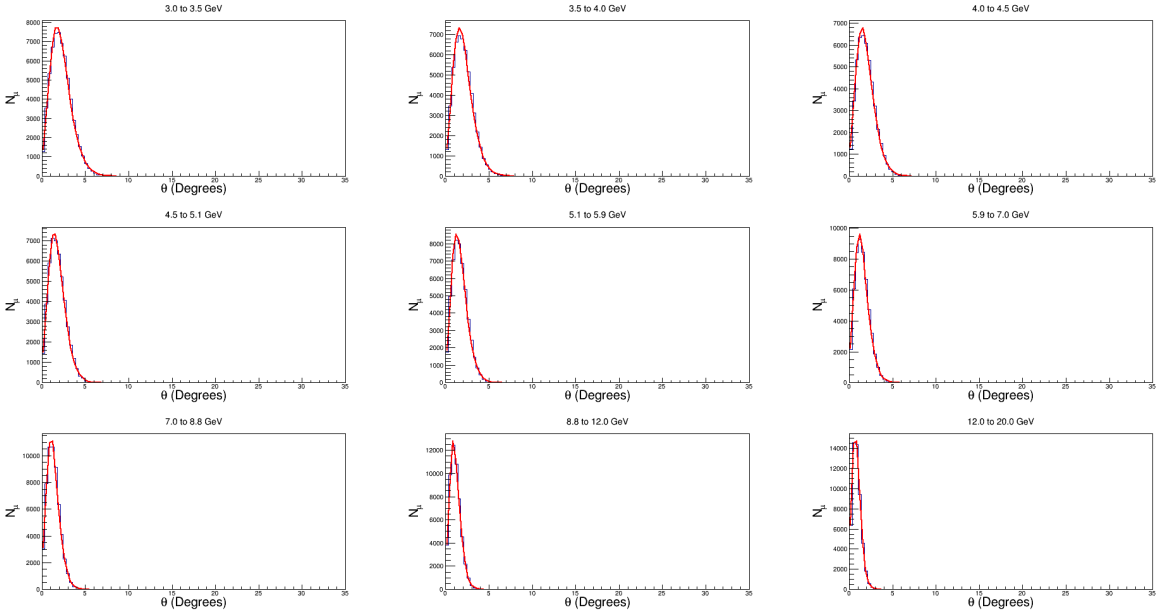

FIGURE 3.7: Number of muons vs θ in different momentum ranges.

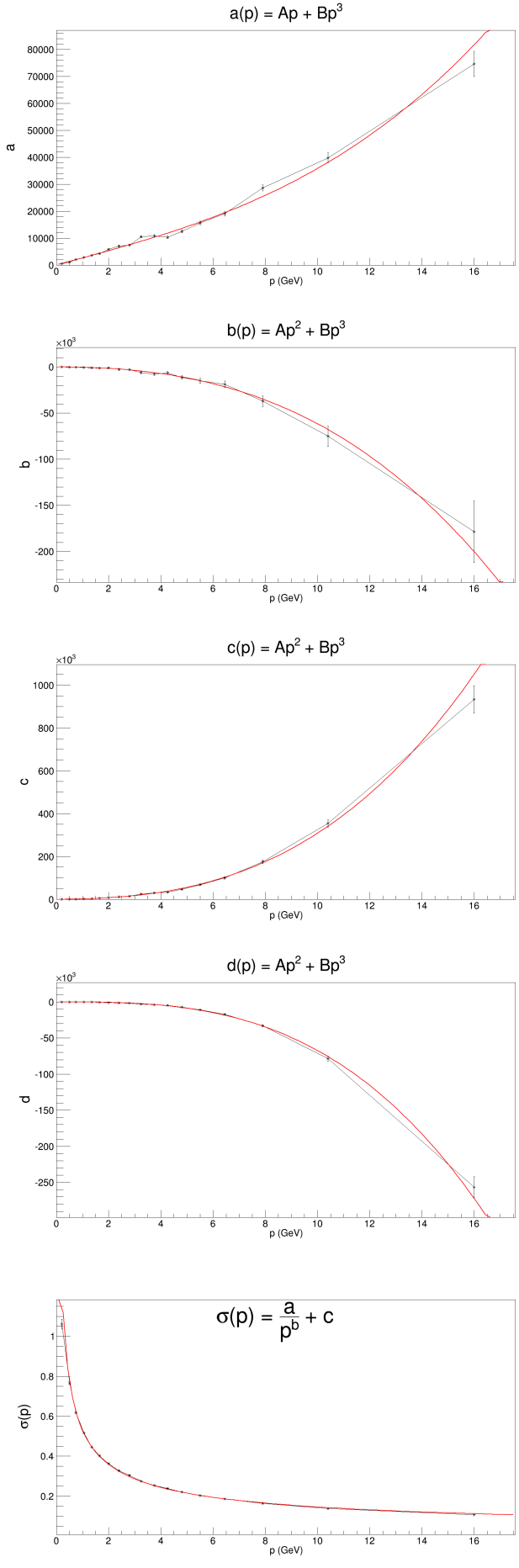

FIGURE 3.8: Plots showing best-fit values for parameters.

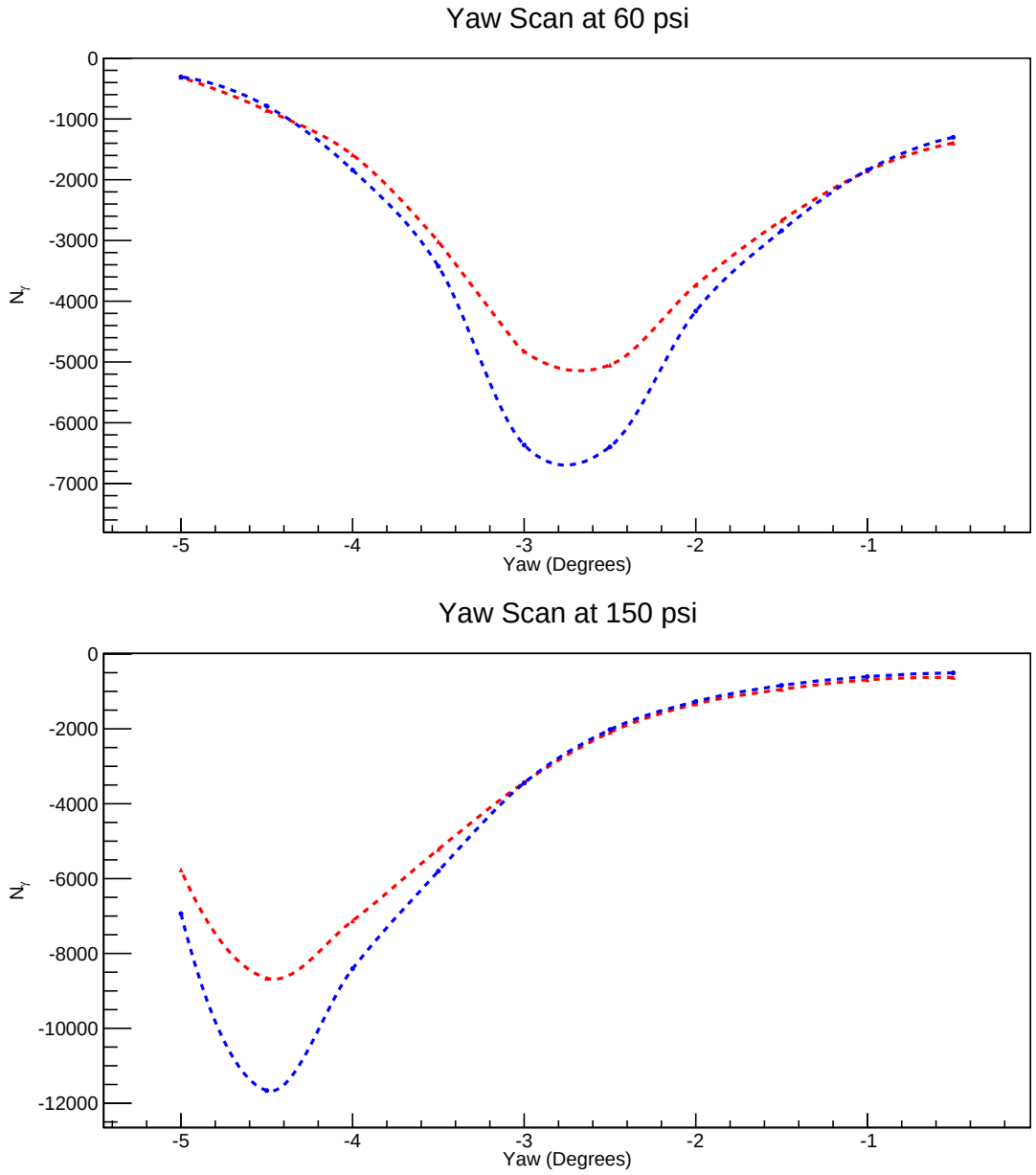

FIGURE 3.9: Yaw scans comparing Monte Carlo simulations (blue) with yield matrix technique (red). The largest disagreement (20%) occurs where the signal is the greatest. This can probably be corrected for better (p, θ) resolution when building the yield matrix.

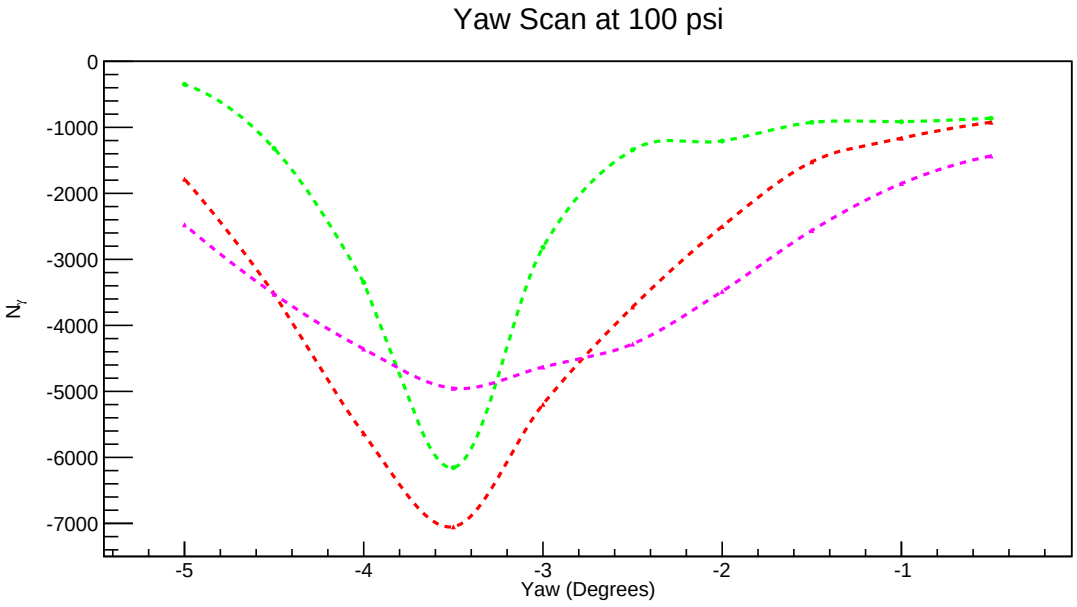

FIGURE 3.10: This plot illustrates how altering the muon distribution (in this case the exponential in Equation 3.2) changes the output signal from a yaw scan. The red line corresponds to a nominal value for the exponent. The green and pink lines correspond to larger and smaller values, respectively, relative to the nominal value. Future work will build upon this model to develop a fitter which matches an output signal with a muon flux.

Chapter 4

Conclusion and Future Work

This thesis has presented the utility of a gas Cherenkov detector for the upcoming DUNE neutrino beam. It has been shown that the detector in the NuMI beamline is able to monitor the beam's stability. Also presented is a method for extracting a muon flux, which would ultimately be used to help constrain the beam's neutrino flux. Although this ultimate goal was not accomplished, the method was proven to be promising. There is no doubt that future work to build upon this model will succeed in characterizing the muon distribution from the output signal.

Although the near detector can be used as a beam monitor, muon monitors accomplish this task much quicker and at a fraction of the cost. Neutrino detection is difficult because they hardly interact and so the near detector relies on a low event rate to monitor the beam. This is not so for muons, they are easy to observe and can measure the beam (as a byproduct of the neutrino beam) much quicker. This will help ensure the beam is working as expected.

Knowing the initial neutrino beam energy spectrum and flavor composition is crucial for DUNE to make accurate measurements of neutrino oscillation parameters. This is also done at the near detector but can be aided with a gas Cherenkov muon detector. Specific muon distributions correspond to unique signals in the detector over several pressures and orientations. A computer model has been developed which will ultimately result in fitting a muon distribution to any given signal. This can be done, in principle, with

Monte Carlo simulations but it would take forever. This paper has shown that generating a muon distribution from some function and turning it into a signal (the fitter would actually do the reverse) saves a significant amount of time.

Future work will be needed to finish this project. The next step would be to develop a fitter which takes a signal (over various detector orientations and pressures) and matches it with some muon distribution according to the functional parameters. This would be done with computer simulations first to make sure the predicted muon flux is accurate. After this, the model will be applied to real data.

Bibliography

[1] *Los Alamos Science No. 25. Celebrating the Neutrino: The Reines-Cowan Experiments* (1997).
http://permalink.lanl.gov/object/tr?what=info:lanl-repo/lareport/LA-UR-97-2534-02.

[2] *European Organization for Nuclear Research (CERN)*. https://home.cern/about/physics/standard-model.

[3] D. Griffiths, *Introduction to Elementary Particles*. Wiley-VCH, 2 ed., 2010.

[4] R. Garisto, *Focus: Neutrinos Have Mass*. Phys. Rev. Focus **2**(10), September 1998. https://physics.aps.org/story/v2/st10.

[5] R. Davis, *Physical Review* **12**(11). 303 (1964).

[6] B. Pontecorvo, *Inverse beta processes and nonconservation of lepton charge*. Soviet Physics JETP (1958).

[7] Z. Maki;M. Nakagawa;S. Sakata, *Remarks on the Unified Model of Elementary Particles*. Progress of Theoretical Physics, Vol. 28, No. 5, November 1962.

[8] D. H. McIntyre *Quantum Mechanics*. Pearson Education Inc.

[9] M. Thomson, *Modern Particle Physics*. Cambridge University Press, 2013.

[10] *Deep Underground Neutrino Experiment*. http://www.dunescience.org/.

[11] Long-Baseline Neutrino Facility. http://lbnf.fnal.gov/beam.html.

[12] Particle Data Group, *Physical Review D: Particles, Fields, Gravitation, and Cosmology*. American Physical Society, July 2012.

[13] P. A. Cherenkov, *Physical Review* **52**(4), 378 (1937).

[14] Bideau-Mehu et al., *Measurement of refractive indices of neon, argon, krypton and xenon*. Journal of Quantitative Spectroscopy and Radiative Transfer, **25**(5), 1981.

[15] J. Boissevain et al., *NuMI Alcove 1 Prototype Cherenkov Muon Monitor*. November 2015.

[16] E. Kemp, *The Deep Underground Neutrino Experiment DUNE: the precision era of neutrino physics*. September 2017. https://arxiv.org/pdf/1709.09385.pdf.

[17] C. Giganti, *Neutrino oscillations: the rise of the PMNS paradigm*. November 2017. https://arxiv.org/pdf/1710.00715.pdf.

[18] P. S. Madigan, *Measuring the muon flux of neutrino beams with a novel gas Cherenkov detector*. November 2015. Undergraduate Honors Theses. Paper 986.

[19] K. Dochen, *Diamond Muon Monitors for the Deep Underground Neutrino Experiment*. April 2017. Undergraduate Honors Theses. Paper 1326.

[20] B. T. Cleveland et al., *Measurement of the Solar Electron Neutrino Flux with the Homestake Chlorine Detector*. American Astronomical Society 496 (March 1998). http://iopscience.iop.org/article/10.1086/305343/pdf.